European Radiology (2019) 29:3424–3430
https://doi.org/10.1007/s00330-019-06245-1

MUSCULOSKELETAL

Milk cloud appearance—a characteristic sign of fibrous dysplasia on contrast-enhanced MR imaging

Daniela Franz[1] · Judith Wechselberger[1] · Michael Rasper[1] · Katja Specht[2,3] · Victoria Kehl[4] · Ernst J. Rummeny[1] · Klaus Woertler[1,3]

Received: 24 January 2019 / Revised: 4 April 2019 / Accepted: 18 April 2019 / Published online: 6 May 2019

Abstract

Objective To evaluate contrast-enhanced T1-weighted magnetic resonance (MR) images in histologically proven fibrous dysplasia (FD) for the prevalence of "milk cloud appearance" and its association with ground-glass appearance (GGA) on radiography or computed tomography (CT).

Methods For this retrospective cohort study, 37 patients with histologically proven FD imaged preoperatively with contrast-enhanced MR imaging and radiography or CT were identified at our institution. Three radiologists independently evaluated MR images for the presence of milk cloud appearance on T1-weighted contrast-enhanced images, sites of skeletal involvement, type of bone involved, uni- vs. multifocality, mono- vs. polyostotic disease, maximum diameter, proportion of bone involved, expansile remodeling, and T2 homogeneity. The presence or absence of GGA on radiography or CT was determined in consensus. Inter-reader agreement was evaluated for milk cloud appearance using Cohen's kappa, and associations between milk cloud appearance and other imaging parameters were tested using Spearman's rho.

Results Among the 37 histologically proven FD lesions, GGA was identified in 70% of the lesions, while milk cloud appearance was found in 82% of the lesions. Inter-reader agreement for milk cloud appearance on MR imaging was good to excellent (κ 0.65, 0.82, and 0.8). A significant correlation was found between milk cloud appearance and GGA ($\rho = 0.31$, $p < 0.001$).

Conclusion Milk cloud appearance is a characteristic sign of FD on contrast-enhanced T1-weighted MR images. Recognition of this feature may be helpful when radiographs are equivocal or unremarkable or when MR imaging is performed as the primary imaging modality in cases of FD.

Key Points

- *Fibrous dysplasia displays a characteristic feature on contrast-enhanced T1-weighted MR imaging: milk cloud appearance.*
- *Milk cloud appearance correlates well with the radiographic or CT finding of ground-glass appearance.*
- *Recognition of milk cloud appearance on contrast-enhanced MR imaging may be helpful when radiographs are equivocal or unremarkable or when MR imaging is performed as the primary imaging modality in cases of fibrous dysplasia.*

Keywords Magnetic resonance imaging · Humans · Radiography · Bone diseases

Abbreviations

CE	Contrast-enhanced
CT	Computed tomography
FD	Fibrous dysplasia
GGA	Ground-glass appearance
MR	Magnetic resonance
T1 TSE	T1-weighted turbo-spin-echo sequence
T2 TSE	T2-weighted turbo-spin-echo sequence
TE	Echo time
TR	Repetition time

✉ Daniela Franz
daniela.franz@tum.de

[1] Department of Diagnostic and Interventional Radiology, School of Medicine, Technical University of Munich, Ismaninger Str. 22, 81675 Munich, Germany

[2] Institute of Pathology, School of Medicine, Technical University of Munich, Munich, Germany

[3] Wilhelm Sander Bone and Soft Tissue Sarcoma Center, Munich, Germany

[4] Institute of Medical Informatics, Statistics and Epidemiology, School of Medicine, Technical University of Munich, Munich, Germany

Introduction

Fibrous dysplasia (FD) is a benign medullary fibro-osseous lesion composed of varying proportions of fibrous tissue and immature woven bone. It occurs in both children and adults without a race or sex predilection [1, 2]. Common sites of skeletal involvement are the femur, the ribs, the craniofacial bones, and the pelvis [1, 3]. Natural history of FD is variable, but malignant transformation is rare [4–6].

A classic imaging sign of FD on computed tomography (CT) and radiographs is the so-called ground-glass appearance (GGA), characterized by a diffusely increased internal density [7]. Magnetic resonance (MR) investigations lack a specific feature. On T1-weighted images, lesions display a non-specific homogeneously hypointense signal, while the appearance on T2-weighted images varies [7, 8]. FD may however be detected incidentally on MR imaging. Hence, a characteristic MR sign of FD, comparable to the GGA on CT/ radiography, would be of great help to classify this incidental finding correctly. Furthermore, when radiographic images of suspected FD are inconclusive, a distinctive MR imaging pattern could help to further evaluate the lesion without exposing the patient to ionizing radiation.

In a considerable proportion of cases referred to our department histologically proven to be FD, we noted a cloudy contrast enhancement pattern within the otherwise low T1 signal of the lesion. The pattern resembles a shot of milk dissolving in tea (Fig. 1a); thus, we called it "milk cloud appearance". Based on this observation, we tested the hypothesis that milk cloud appearance represents a characteristic feature of FD on contrast-enhanced T1-weighted MR images.

The purpose of this retrospective study was to review imaging studies of a series of histologically proven FD lesions in order to determine the prevalence of milk cloud appearance on contrast-enhanced T1-weighted MR imaging and to evaluate a possible association with GGA on radiography or CT.

Materials and methods

Subjects

For this retrospective cohort study, institutional review board approval was obtained and the requirement for informed patient consent was waived due to the retrospective nature of the study. All consecutive subjects with a histologically proven diagnosis of FD who had undergone preoperative CT or radiography and contrast-enhanced MR imaging between March 2007 and June 2017 were retrieved from the institutional database and reviewed, resulting in a total of 37 subjects. Thirty-seven histologically proven FD lesions were analyzed in those 37 patients including 21 female patients (57%). Mean age was 32.1 ± 14.4 years (range, 11–60 years) at diagnosis, with a mean age of 31.1 years (range, 11–60 years) in males and a mean age of 33.2 years (range, 12–59 years) in females. Image analysis was performed using pseudonymized data.

Image acquisition

At our institution, MR images were acquired on a 1.5-T system (Avanto; Siemens Healthcare) or on a 3.0-T system (Verio; Siemens Healthcare or Ingenia; Philips Healthcare). In all patients, including patients imaged at other institutions, MR imaging protocols included at least three sequences in not less than two standard imaging planes (axial and coronal or sagittal) with at least one T2-weighted sequence without fat suppression and at least one T1-weighted sequence before and after intravenous administration of a gadolinium chelate. Typical sequence parameters were as follows: for 1.5-T systems: T1-weighted turbo-spin-echo sequence (T1 TSE): repetition time (TR) = 395–630 ms, echo time (TE) = 8–14 ms, T2-weighted turbo-spin-echo sequence (T2 TSE): TR = 3235–7830 ms, TE = 85–120 msec; for 3-T systems: T1 TSE: TR = 488–744 ms, TE = 12–30 ms, T2 TSE: TR = 1380–5824 ms, TE = 70–99 ms. T1-weighted sequences after contrast administration were performed with or without fat suppression. In patients imaged without fat suppression, subtraction images were calculated from the T1-weighted images before and after contrast administration.

Image analysis

Image datasets were analyzed by three radiologists with expertise in musculoskeletal imaging (K.W., 25 years; M.R., 7 years; and J.W., 8 years of experience). The histologically proven lesion in each patient was defined as the target lesion. On radiography or CT of the target lesions, GGA was defined as a homogeneous, intermediate opacity/attenuation between that of normal cortical bone and soft tissue (Fig. 1b), comparable to the matte finish of glass stoppers used in laboratory glassware. The presence of GGA was determined in consensus.

On MR imaging, milk cloud appearance was defined as a cloudy pattern of contrast enhancement on T1-weighted MR sequences involving the entire lesion, or the entire solid portion of the lesion if cystic components were present.

All MR images were analyzed independently by each of the three readers for the following criteria:

1. Presence or absence of milk cloud appearance on T1-weighted contrast-enhanced MR images of the target lesion with the definition of milk cloud appearance as described above.
2. Sites of skeletal involvement: Readers named the bone involved by the histologically proven lesion. Bones were then divided into two categories: long bones and other bone types. Long bones included the humerus, radius, ulna, femur, fibula, tibia, metatarsal bones, and phalanges.

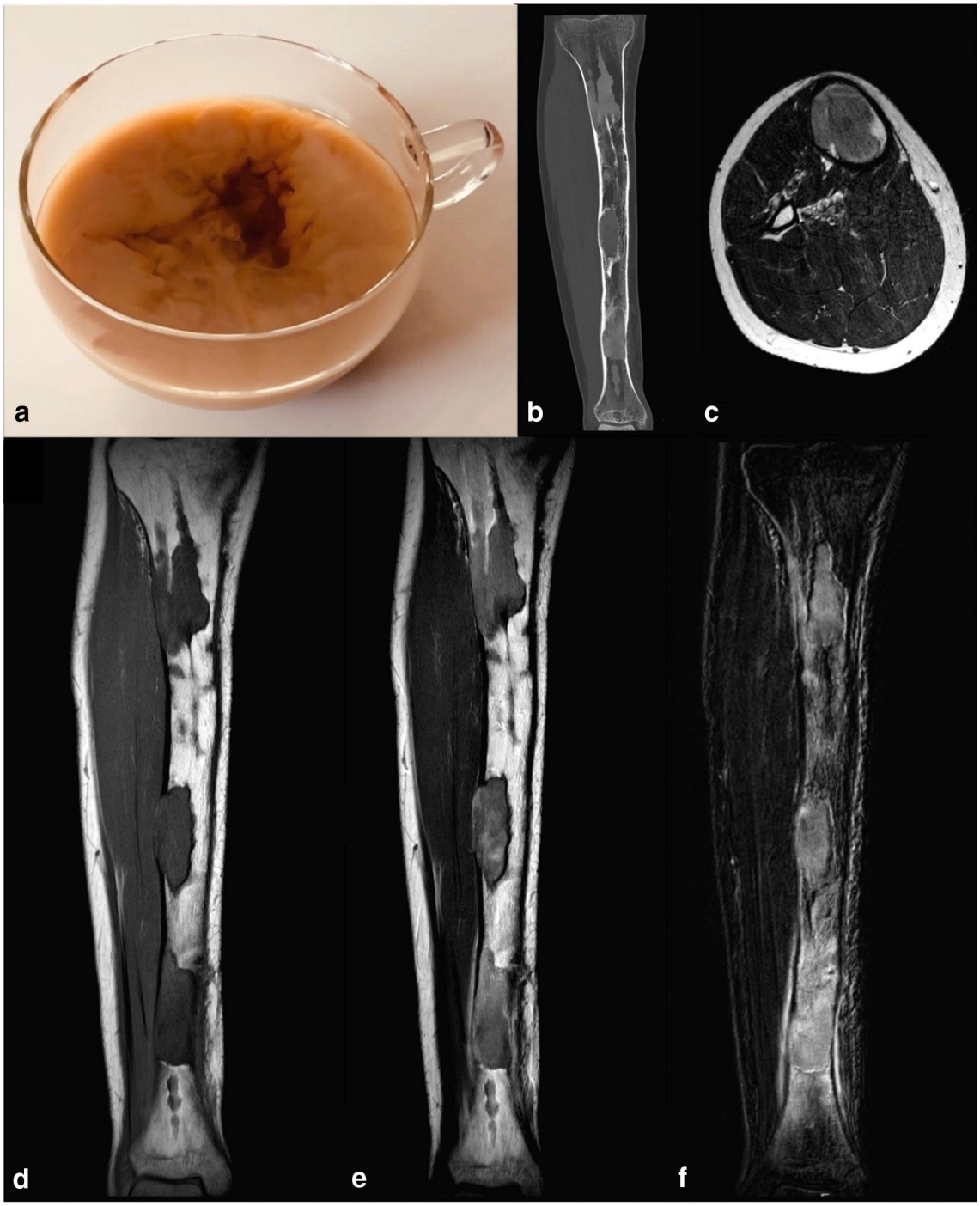

Fig. 1 **a** A shot of milk in tea dissolving in a pattern of a cloud. **b** Coronal reformation of a CT of a lower leg exhibiting multifocal ground-glass lesions throughout the tibial diaphysis in an 11-year-old male patient with histologically proven FD. **c** Axial T2-weighted MR image displaying low signal intensity of the midshaft lesion. **d** Coronal T1-weighted MR image shows a homogeneously hypointense signal within the lesions. Corresponding coronal contrast-enhanced T1-weighted MR image (**e**) and subtraction image (**f**) of the tibia both display milk cloud appearance throughout all lesions. CT, computed tomography; FD, fibrous dysplasia; MR, magnetic resonance

3. Uni- vs. multifocality: Available images were checked for multiple lesions similar to the target lesion within one bone. If only one lesion was found within the site of skeletal involvement, the readers rated the FD as unifocal, in cases with multiple lesions as multifocal.
4. Mono- vs. polyostotic disease: Available images were checked for lesions similar to the target lesion in different bones. If lesions in two or more bones were found, the FD was rated as polyostotic, otherwise as monostotic. If no full-body imaging was available, type of FD was rated unknown.

5. Maximum diameter: Readers measured the maximum diameter of the target lesion using the plane depicting the lesion in its greatest extent. The diameter was recorded in millimeters.
6. Proportion of the bone involved: Readers estimated the proportion of the bone involved by the target lesion. Graduation was defined as up to 30% of the bone, up to 50%, or more than 50% of the bone.
7. Expansile remodeling (yes/no): Expansile remodeling was defined as the lesion leading to deformation and an increase in the volume of the involved bone.
8. T2 homogeneity (yes/no) on MR imaging: The target lesion was rated based on its homogeneity on T2-weighted MR images.

Histopathological analysis

Histology was reviewed by a soft tissue and bone pathologist (K.S.). In addition to the confirmation of the diagnosis of FD according to the generally accepted criteria [1], the presence of specific histopathological patterns was determined as suggested by [9]: classical pattern, fatty metamorphosis, myxoid stroma, collagenization of stroma, stroma-rich pattern, foam cells, calcified spherules, osteoblastic rimming.

Statistical analysis

Statistical analysis was performed under the supervision of a statistician (V.K.). Data are expressed as mean ± standard deviation (SD) (with range in parentheses). The relationship between the presence of milk cloud appearance and the characteristics of FD was tested using the Spearman rank correlation coefficient. The inter-reader agreement for milk cloud appearance was evaluated with Cohen's kappa coefficient, expressed as κ, with 95% confidence interval (CI) in parentheses. Inter-reader agreement was interpreted as excellent ($\kappa > 0.81$), good ($\kappa = 0.61$–0.80), moderate ($\kappa = 0.41$–0.60), fair ($\kappa = 0.21$–0.40), or poor ($\kappa \leq 0.20$) [10]. No formal adjustments for multiple testing were done due to the explorative character of the study; however, the significance level was set at 1%. Statistical analysis was performed using MedCalc Statistical Software (version 18.11.3; MedCalc Software bvba; 2019).

Results

The 37 target lesions had the following skeletal distribution: femur (15 lesions, 41%), pelvis (8, 22%), tibia (5, 14%), ribs (4, 11%), metatarsal bone (2, 5%), and lumbar spine, radius, and skull (1 lesion, 3% each). Twenty-three of the lesions were located in long bones (62%) and the remaining 14 (38%) in other skeletal elements. Seven cases (19%) were multifocal, the remaining unifocal. Three cases (8%) were cases of monostotic FD, seven cases (19%) were polyostotic FD, and the remaining 27 cases (73%) could not be classified as no whole-body imaging had been performed. The longest maximum diameter of target lesions was measured on average at 92.9 mm ± 81.8 mm (range, 15–360 mm). Twenty-three target lesions (62%) involved less than 30% of the bone, 6 cases (16%) involved up to 50% of the bone, and 8 lesions (22%) involved more than 50% of the bone. Twenty-two target lesions (59%) showed expansile remodeling and 10 lesions (27%) appeared homogeneous on T2-weighted images.

In 19 lesions, CT was available, while for the remaining 18 lesions, only radiographs were available. A total of 26 lesions (70%; 10 on CT and 16 on radiography) displayed characteristic GGA.

Milk cloud appearance on contrast-enhanced T1-weighted MR images was found in 82% of the lesions. Inter-reader agreement for the detection of milk cloud appearance was good to excellent with $\kappa = 0.65$ (95% CI 0.34–0.96), $\kappa = 0.82$ (95% CI 0.59–1.0), and $\kappa = 0.8$ (95% CI 0.54–1.0), respectively.

The Spearman rank correlation coefficient between milk cloud appearance on contrast-enhanced T1-weighted MR images and GGA on radiography or CT resulted in an association ($\rho = 0.31$) which was highly statistically significant ($p < 0.001$). In patients presenting both GGA on radiography or CT and milk cloud appearance on MR imaging (63% of cases), bone segments with milk cloud appearance were always co-localized with the segments with GGA (Figs. 1, 2, and 3). Milk cloud appearance on contrast-enhanced T1-weighted MR imaging had a higher prevalence in lesions located in long bones than in other bones (91% vs. 67%, respectively, see Fig. 2), and a significant correlation between milk cloud appearance and the type of bone was found ($\rho = 0.31$, $p < 0.001$). No other associations were identified between the presence of milk cloud appearance and the characteristics of FD (Table 1).

Review of histology samples confirmed the diagnosis of FD in all cases. A classical pattern was found in 50% of the lesions, fatty metamorphosis in 29%, myxoid stroma in 32%, collagenization of stroma in 26%, stroma-rich pattern in 41%, foam cells in 15%, calcified spherules in 24%, and osteoblastic rimming in 21% of the lesions. The Spearman rank correlation coefficient for the association between milk cloud appearance on contrast-enhanced T1-weighted MR images and the histologic patterns revealed an inverse association between fatty metamorphosis and milk cloud appearance ($\rho = -0.35$, $p < 0.001$; Table 2).

Discussion

The present study found a majority of histologically proven cases of FD to display a characteristic contrast enhancement pattern on T1-weighted MR imaging: milk cloud appearance.

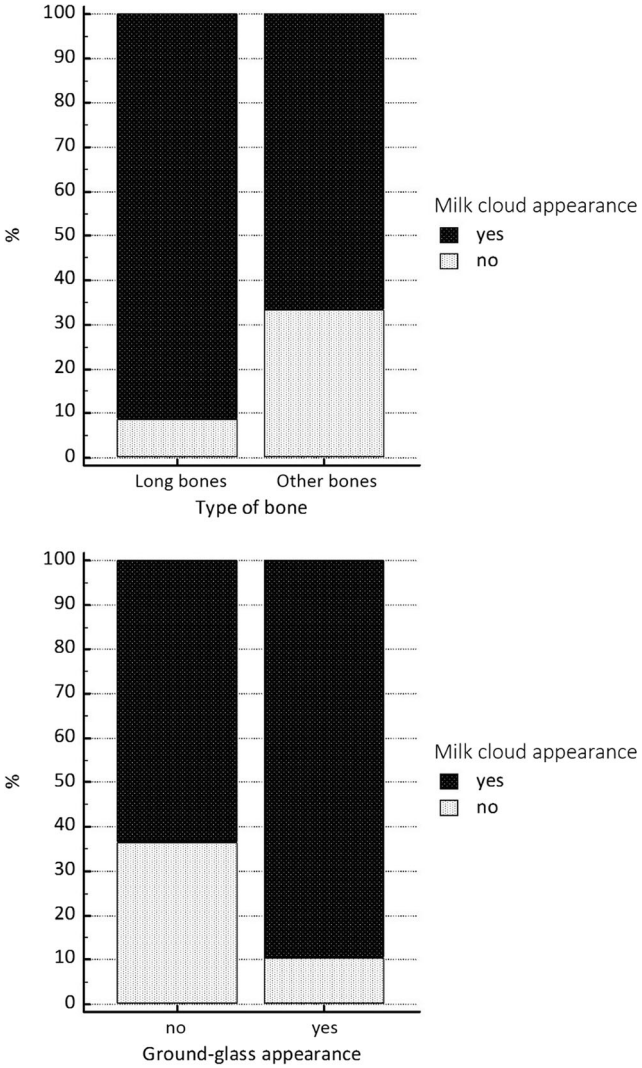

Fig. 2 Frequency charts: (**a**) Histologically proven FD lesions with and without ground-glass appearance on radiography or CT and corresponding frequencies of milk cloud appearance on contrast-enhanced T1-weighted MR imaging. **b** Histologically proven FD lesions in long bones and other bone types and corresponding frequencies of milk cloud appearance on contrast-enhanced T1-weighted MR imaging. FD, fibrous dysplasia; CT, computed tomography; MR, magnetic resonance

The detection of milk cloud appearance correlated with the presence of GGA on radiography and CT. Furthermore, milk cloud appearance was more prevalent in FD located in long bones than in other skeletal sites.

Timely diagnosis of FD is critical in order to avoid unnecessary diagnostic procedures and to initiate appropriate management. MR imaging is an increasingly common imaging modality. However, to date, no specific MR imaging characteristics of FD have been described.

MR imaging features of FD described in the literature are non-specific and variable. The fibrous tissue might cause low-intensity signals often seen on T1-weighted sequences. On T2-weighted sequences, FD displays variable signal intensities, consistent with the degree of fibrous tissue, bone formation, and cystic or hemorrhagic changes of the lesion [2, 8, 11, 12]. According to previous studies, FD demonstrates varying degrees of enhancement after intravenous contrast application. Shah et al described enhancement patterns in 15 cases as a patchy central, rim or homogeneous enhancement, or a combination [13], while an earlier study reported central and peripheral rim enhancement in a total of 11 cases [7].

In the present study, GGA was found in the majority of histologically proven FD lesions on radiography or CT. However, almost one-third of the evaluated lesions did not display GGA, and milk cloud appearance on contrast-enhanced T1-weighted MR images could be identified more frequently than GGA. In lesions presenting both GGA and milk cloud appearance, the localization of both appearances correlated well. During their natural progression, FD lesions exhibit fibrous stroma and immature woven bone, with the hallmark of FD being an inability to produce mature lamellar bone [14]. More dense tissue with prominent cement lines can be found in older lesions [3]. GGA results from a closely meshed, fine spicular component of the woven bone within the lesion [15]. When following up a maxillofacial FD lesion with CT, Tokano et al described an "onion peel"–like structure at primary diagnosis, then after 2 years, the authors describe the CT appearance to be that of an "eggshell lesion" with peripheral calcifications, and only over the course of the next 3 years, GGA became evident [16]. Thus, it could be postulated that GGA occurs at later stages of the natural progression of FD while milk cloud appearance possibly represents an earlier finding, independent of the presence of woven bone within the lesion as compared to GGA.

Milk cloud appearance was more prevalent in FD located in long bones compared with other skeletal sites. One possible explanation is the site-specific differences in the histological pattern of FD, as described by Riminucci et al [17]. However, those differences were mainly found between cranial/gnathic bones and limb/axial skeleton bones. Nevertheless, when regarding FD as a stem cell disease [18], the differences in the cellular composition of bone site-specific marrow [19] might be a reason for FD displaying different contrast enhancement patterns in long bones compared with other skeletal sites.

The exact etiology of milk cloud appearance remains unknown. According to Utz et al, FD is a well-vascularized lesion with numerous small vessels in the center and with large peripheral sinusoids [8], while Parekh et al described the lesions to be composed of a fibrous stroma that is usually avascular [14]. One theory would be that fibrous tissue is responsible for the pattern of contrast enhancement seen on T1-weighted contrast-enhanced MR images in the present study. Shidham et al described varying stromal patterns observed in fibrous dysplasia, including the previously unreported fatty metamorphosis [9]. In the present study, milk cloud appearance on MR imaging was observed less frequently in

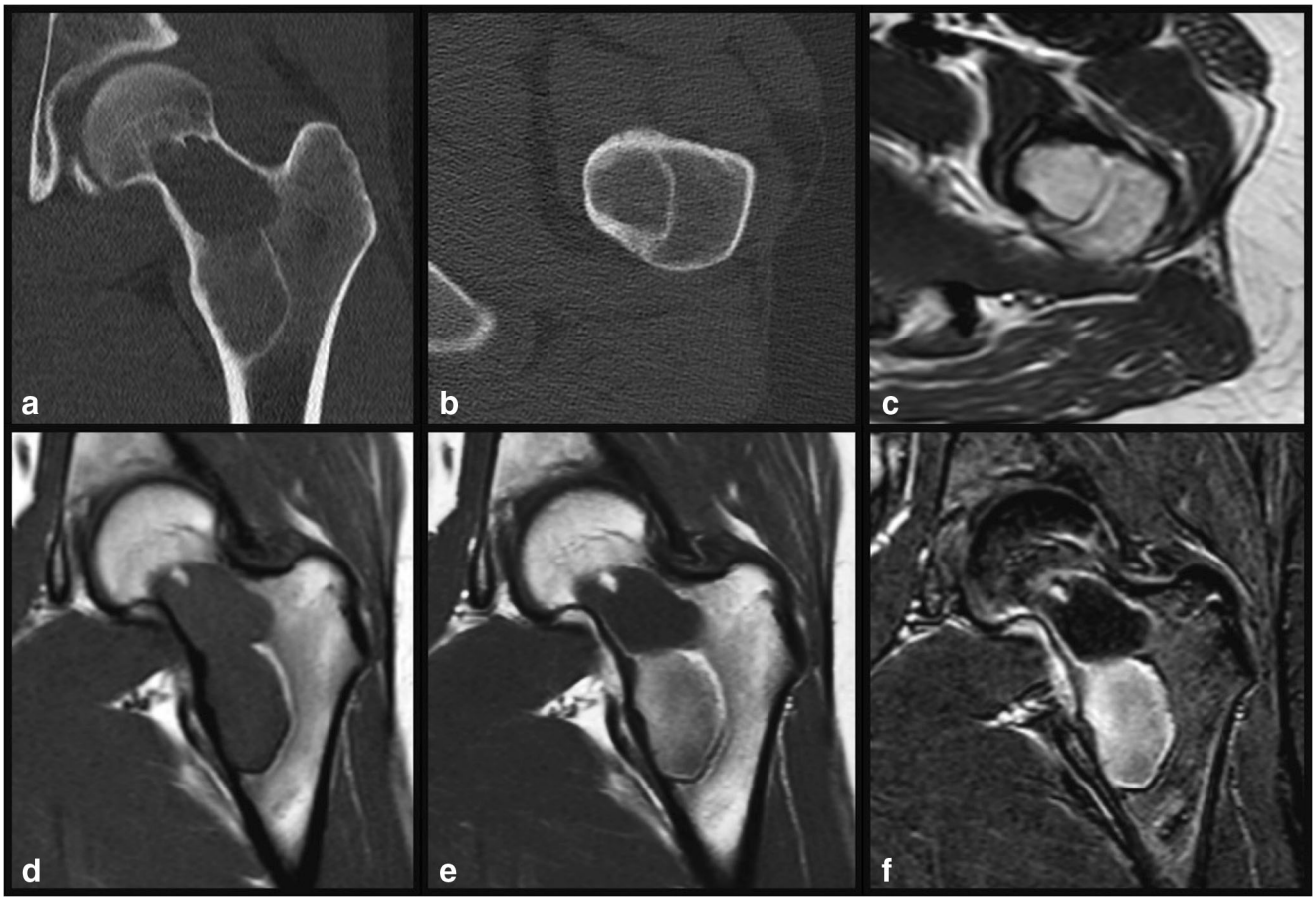

Fig. 3 **a** Coronal CT of the left hip in a 17-year-old female patient with histologically proven FD exhibiting a lesion with ground-glass appearance around the lesser trochanter next to a purely lytic part in the femoral neck. **b** Transverse reformation image of the ground-glass area displaying no cortical destruction. **c** Transverse T2-weighted MR image showing a non-specific intermediate signal intensity of the ground-glass area of the lesion. **d** Unenhanced coronal T1-weighted MR image of the lesion, displaying similar low signal intensities of the lytic and the ground-glass area. Corresponding coronal contrast-enhanced T1-weighted MR image (**e**) and subtraction image (**f**). Note the milk cloud appearance within the corresponding area of ground-glass appearance on CT. The lytic part of the lesion shows no contrast enhancement. FD, fibrous dysplasia; CT, computed tomography; MR, magnetic resonance

those lesions exhibiting fatty metamorphosis. However, no significant positive correlation was found between milk cloud appearance and specific histology patterns.

The patient population in this study is representative of the classic population presenting with FD. The young age at presentation, the lack of a clear sex predilection, and the skeletal

Table 1 Association between the presence of milk cloud appearance on T1-weighted contrast-enhanced MR images and other characteristics of fibrous dysplasia

Parameter	Spearman's coefficient of rank correlation (rho)	*p* values
Patient age (years)	0.08	0.40 (n.s.)
Sex (male/female)	0.23	0.02 (n.s.)
Ground-glass appearance on CT or radiography (yes/no)	0.31	< 0.001
Type of bone (long bone/other)	0.31	< 0.001
Involvement pattern (uni-/multifocal)	0.05	0.62 (n.s.)
Disease type (mono-/ polyostotic)	0.03	0.77 (n.s.)
Maximum diameter (mm)	0.20	0.04 (n.s.)
Proportion of bone involved (%)	0.15	0.12 (n.s.)
Expansile remodeling (yes/no)	0.18	0.06 (n.s.)
Homogeneity on T2-weighted MR images (yes/no)	0.12	0.24 (n.s.)

CT, computed tomography; *MR*, magnetic resonance; *n.s.*, non-significant

Table 2 Association between the presence of milk cloud appearance on T1-weighted contrast-enhanced MR images and the presence of specific histology patterns

Histologic pattern	Spearman's coefficient of rank correlation (rho)	*p* values
Classical pattern	− 0.08	0.45 (n.s.)
Fatty morphogenesis	− 0.35	< 0.001
Myxoid stroma	− 0.11	0.28 (n.s.)
Collagenization of stroma	0.03	0.78 (n.s.)
Stroma-rich pattern	− 0.18	0.07 (n.s.)
Foam cells	− 0.08	0.44 (n.s.)
Calcified spherules	0.22	0.03 (n.s.)
Osteoblastic rimming	− 0.25	0.01 (n.s.)

MR, magnetic resonance; *n.s.*, non-significant

distribution of the lesions evaluated in the present study are in line with previous reports [3, 15].

Our study has some limitations. First, a direct co-localization of the areas with milk cloud appearance with histology was not possible due to the retrospective nature of the study. Second, due to the study design without a control group comprising other tumor entities, the sensitivity and specificity of milk cloud appearance for detection of FD cannot be calculated, and overlap with MR-findings of other bone lesions cannot be excluded. Validation in a larger cohort with a control group and blinded reading regarding histopathologic confirmation will have to be performed in order to evaluate whether milk cloud appearance is pathognomonic for FD.

In conclusion, FD displays a characteristic feature on contrast-enhanced T1-weighted MR imaging, which correlates well with the radiographic or CT finding of GGA: milk cloud appearance. Recognition of this sign may be helpful when radiographs are equivocal or unremarkable or when MR imaging is performed as the primary imaging modality in cases of FD.

Funding The authors state that this work has not received any funding.

Compliance with ethical standards

Guarantor The scientific guarantor of this publication is Prof. Klaus Woertler.

Conflict of interest The authors of this manuscript declare no relationships with any companies whose products or services may be related to the subject matter of the article.

Statistics and biometry Victoria Kehl kindly provided statistical advice for this manuscript.

Informed consent Written informed consent was waived by the Institutional Review Board.

Ethical approval Institutional Review Board approval was obtained.

Methodology
- Retrospective
- Cross-sectional study
- Performed at one institution

References

1. Fletcher CDM, Bridge JA, Hogendoorn P, Mertens F (2013) WHO classification of tumours of soft tissue and bone, 4th edn. IARC Press
2. DiCaprio MR, Enneking WF (2005) Fibrous dysplasia. Pathophysiology, evaluation, and treatment. J Bone Joint Surg Am 87:1848–1864
3. Forest M, Tomeno B, Vanel D (1998) Orthopedic surgical pathology: diagnosis of tumors and pseudotumoral lesions of bone and joints. Churchill Livingstone
4. Henry A (1969) Monostotic fibrous dysplasia. J Bone Joint Surg Br 51:300–306
5. Grabias SL, Campbell CJ (1977) Fibrous dysplasia. Orthop Clin North Am 8:771–783
6. Schwartz DT, Alpert M (1964) The malignant transformation of fibrous dysplasia. Am J Med Sci 247:1–20
7. Jee WH, Choi KH, Choe BY, Park JM, Shinn KS (1996) Fibrous dysplasia: MR imaging characteristics with radiopathologic correlation. AJR Am J Roentgenol 167:1523–1527
8. Utz JA, Kransdorf MJ, Jelinek JS, Moser RP Jr, Berrey BH (1989) MR appearance of fibrous dysplasia. J Comput Assist Tomogr 13:845–851
9. Shidham VB, Chavan A, Rao RN, Komorowski RA, Asma Z (2003) Fatty metamorphosis and other patterns in fibrous dysplasia. BMC Musculoskelet Disord 4:20
10. Landis JR, Koch GG (1977) The measurement of observer agreement for categorical data. Biometrics 33:159–174
11. Fisher AJ, Totty WG, Kyriakos M (1994) MR appearance of cystic fibrous dysplasia. J Comput Assist Tomogr 18:315–318
12. Fitzpatrick KA, Taljanovic MS, Speer DP et al (2004) Imaging findings of fibrous dysplasia with histopathologic and intraoperative correlation. AJR Am J Roentgenol 182:1389–1398
13. Shah ZK, Peh WC, Koh WL, Shek TW (2005) Magnetic resonance imaging appearances of fibrous dysplasia. Br J Radiol 78:1104–1115
14. Parekh SG, Donthineni-Rao R, Ricchetti E, Lackman RD (2004) Fibrous dysplasia. J Am Acad Orthop Surg 12:305–313
15. Kransdorf MJ, Moser RP Jr, Gilkey FW (1990) Fibrous dysplasia. Radiographics 10:519–537
16. Tokano H, Sugimoto T, Noguchi Y, Kitamura K (2001) Sequential computed tomography images demonstrating characteristic changes in fibrous dysplasia. J Laryngol Otol 115:757–759
17. Riminucci M, Liu B, Corsi A et al (1999) The histopathology of fibrous dysplasia of bone in patients with activating mutations of the Gs alpha gene: site-specific patterns and recurrent histological hallmarks. J Pathol 187:249–258
18. Riminucci M, Saggio I, Robey PG, Bianco P (2006) Fibrous dysplasia as a stem cell disease. J Bone Miner Res 21(Suppl 2):P125–P131
19. de Souza Faloni AP, Schoenmaker T, Azari A et al (2011) Jaw and long bone marrows have a different osteoclastogenic potential. Calcif Tissue Int 88:63–74